Development 136, 3235-3246 (2009) doi:10.1242/dev.037028

Regulation of preprocambial cell state acquisition by auxin signaling in *Arabidopsis* leaves

Tyler J. Donner, Ira Sherr and Enrico Scarpella*

The principles underlying the formation of veins in the leaf have long intrigued developmental biologists. In *Arabidopsis* leaves, files of anatomically inconspicuous subepidermal cells that will elongate into vein-forming procambial cells selectively activate *ATHB8* gene expression. The biological role of *ATHB8* in vein formation and the molecular events that culminate in acquisition of the *ATHB8* preprocambial cell state are unknown, but intertwined pathways of auxin transport and signal transduction have been implicated in defining paths of vascular strand differentiation. Here we show that *ATHB8* is required to stabilize preprocambial cell specification against auxin transport perturbations, to restrict preprocambial cell state acquisition to narrow fields and to coordinate procambium formation within and between veins. We further show that *ATHB8* expression at preprocambial stages is directly and positively controlled by the auxin-response transcription factor MONOPTEROS (MP) through an auxin-response element in the *ATHB8* promoter. We finally show that the consequences of loss of *ATHB8* function for vein formation are masked by *MP* activity. Our observations define, at the molecular level, patterning inputs of auxin signaling in vein formation.

KEY WORDS: *Arabidopsis thaliana*, Leaf development, Vascular patterning, Vein formation, Procambium, Auxin signal transduction, Auxin transport, *ATHB8*, *MONOPTEROS*

INTRODUCTION

The vascular system of plants is composed of bundles of cell files that extend and intersect throughout all organs (Esau, 1965). Vascular bundles differentiate from procambial cells: narrow, cytoplasm-dense cells, characteristically arranged in continuous strands (Esau, 1943), which in leaves seem to emerge de novo from within the morphologically homogeneous population of apparently naïve ground cells (Foster, 1952; Pray, 1955).

Although the molecular details are not entirely clear, a role for the polarly transported plant signaling molecule auxin in the selection of leaf ground cells that will elongate to acquire procambial cell identity has increasingly gained experimental support (Mattsson et al., 2003; Mattsson et al., 1999; Sachs, 1981; Sachs, 1989; Scarpella et al., 2006; Sieburth, 1999; Wenzel et al., 2007). During leaf development, polygonal, isodiametric ground cells are shunted towards procambial fate through induction of broad domains of expression of the PIN1 auxin exporter (Scarpella et al., 2006; Wenzel et al., 2007). Decay of PIN1 expression and associated relapse to ground state occur in some of the cells initially expressing PIN1, and domains of PIN1 expression are eventually curtailed to individual files of cells that will stretch into procambial cells (Scarpella et al., 2006; Wenzel et al., 2007). Because formation of leaf vascular bundles, or veins, is reiteratively propagated in leaf development (reviewed by Nelson and Dengler, 1997), cells that have reverted to ground state may have other opportunities to assume procambial identity before adopting the alternative mesophyll fate (Scarpella et al., 2004; Scarpella et al., 2006; Wenzel et al., 2007).

While onset of PIN1 expression marks an unstable and reversible state in vein formation, files of PIN1-expressing ground cells that are stabilized towards procambial fate initiate expression of the homeodomain-leucine zipper (HD-Zip) III gene *ATHB8* (Baima et al., 1995; Kang and Dengler, 2004; Sawchuk et al., 2007; Scarpella et al., 2004). Available evidence suggests that *ATHB8* expression identifies a crucial and typically irreversible stage in procambial cell fate acquisition: under both undisturbed and perturbed conditions, adoption of the *ATHB8* 'preprocambial' cell state accurately predicts sites of vascular differentiation (Alonso-Peral et al., 2006; Carland and Nelson, 2004; Cnops et al., 2006; Kang and Dengler, 2004; Koizumi et al., 2000; Petricka and Nelson, 2007; Pineau et al., 2005; Sawchuk et al., 2007; Scarpella et al., 2004; Scarpella et al., 2006), and the *ATHB8* preprocambial state is mutually exclusive with a 'premesophyll' cell state that presages mesophyll fate assignment (Sawchuk et al., 2008). Whereas the preprocambial state is defined by the onset of *ATHB8* expression, differential *ATHB8* expression is only the object of a cell state transition and therefore does not necessarily provide information about the underlying patterning mechanism. Instead, knowledge of the set of transcription factors that determine initiation of *ATHB8* expression at the correct spatiotemporal coordinates in leaf development might provide insight into how the preprocambial cell state arises at defined positions and stages during leaf development.

Here, we show that *ATHB8* is required to stabilize preprocambial cell specification against auxin transport perturbations, to constrict preprocambial cell state acquisition to narrow zones and to synchronize procambial cell identity assignment within and between veins. Further, we show that *ATHB8* preprocambial expression is directly and positively controlled by the auxin-response transcription factor MONOPTEROS (MP) through an auxin-response element in the *ATHB8* promoter. Finally, we show that *ATHB8* functions in vein formation strictly depend on *MP* activity. Our results suggest a molecular mechanism through which general auxin signal transduction is specifically translated into leaf vascular patterning inputs.

MATERIALS AND METHODS

Vector construction

Sequences of primers and details of cloning are available on request. To generate the DR5Rev(9x)$_{pro}$:ECFP-Nuc construct, nine copies of the DR5Rev sequence (Ulmasov et al., 1997) upstream of the –46 cauliflower

Department of Biological Sciences, University of Alberta, CW-405 Biological Sciences Building, Edmonton AB, T6G 2E9, Canada.

*Author for correspondence (enricos@ualberta.ca)

Accepted 31 July 2009

mosaic virus 35S promoter (Fang et al., 1989) were recombined into the pBGCN vector (Kubo et al., 2005). To generate the $ATHB8_{pro}$:ATHB8:mCherry construct, the mCherry coding sequence (Shaner et al., 2004) was cloned downstream of the fragment of the *ATHB8* gene from –1997 to +4233. Functionality of the construct was tested by transformation into homozygous *athb8-11* plants and by assessing normalization of sensitivity towards 5 μM 1-N-naphthylphthalamic acid (NPA; Sigma Aldrich, St Louis, MO, USA) in two independent, single-insertion transgenic lines. To generate the *ATHB8* promoter deletion and mutation constructs, amplified fragments were recombined into the pFYTAG vector (Zhang et al., 2005). To generate the MP_{pro}:MP:ECFP construct, the ECFP coding sequence (Clontech Laboratories, Mountain View, CA, USA) was cloned at position +3815 of the fragment of the *MP* gene from –3311 to +4301. Functionality of the construct was tested by crossing two independent, single-insertion lines to heterozygous mp^{U55} plants and by assessing rescue of the root phenotype in the F2 generation. To generate the $UBQ10_{pro}$:MP:GR construct, the sequence encoding amino acids 508-795 of the rat glucocorticoid receptor (Sablowski and Meyerowitz, 1998) was cloned downstream of the fragment of the *MP* cDNA (Hardtke and Berleth, 1998) from +1 to +2696 and controlled by the *UBQ10* promoter (Sawchuk et al., 2008).

Plant material and growth conditions

The origins of the $PIN1_{pro}$:PIN1:EYFP, J1721:mGFP5er, Q0990:mGFP5er, $ATHB8_{pro}$:HTA6:EYFP, $UBQ10_{pro}$:EGFP:LTi6b, $ATHB8_{pro}$:ECFP-Nuc, *athb8-11* and *athb8-12* lines have been published (Xu et al., 2006; Sawchuk et al., 2007; Sawchuk et al., 2008; Prigge et al., 2005). The mp^{U55} line contains a G-to-A transition at position +1237 that disrupts the splicing acceptor site of the sixth intron and is predicted to result in loss of sequences strictly required for DNA binding (Ulmasov et al., 1999). The proportion of mp^{U55} seedlings with single cotyledons (55/116, 47%), fused cotyledons (27/116, 23%) and two cotyledons (34/116, 29%) meet established criteria that define strong *mp* alleles (Berleth and Jurgens, 1993). Therefore, both molecular and morphological evidence indicate the extreme severity of the mp^{U55} mutation. The SALK_021319 line was confirmed to contain a single T-DNA insertion at position +3422 of the *MP* (*ARF5*) gene and was therefore renamed *arf5-2*. Sequences of primers used for genotyping are available on request.

Seeds were sterilized and germinated, and seedlings and plants were grown, transformed and selected as described (Sawchuk et al., 2008; Sawchuk et al., 2007). For auxin transport inhibition, seeds were germinated on growth medium supplemented with NPA. For auxin or dexamethasone induction, seeds were germinated on growth medium, transferred at 3.5 days after germination (DAG) to liquid growth medium supplemented with 10 μM 2,4-dichlorophenoxyacetic acid (Sigma Aldrich) or 30 μM dexamethasone (Sigma Aldrich) and incubated with shaking at 50 rpm under normal growth conditions for 16 hours prior to imaging.

Microtechniques and microscopy

Dissected leaf primordia were mounted and imaged as described (Sawchuk et al., 2008; Sawchuk et al., 2007). Detailed information on imaging parameters is available upon request. To visualize xylem patterns, leaves were cleared as described (Scarpella et al., 2004) and viewed under dark-field illumination with an Olympus SZ61TR stereomicroscope (Olympus Corporation, Tokyo, Japan). Images were captured with an AxioCam HR camera (Carl Zeiss, Oberkochen, Germany).

Image analysis and processing

Brightness and contrast were not altered for images of mock treatments and induced gene expression. For all other images, brightness and contrast were adjusted through linear stretching of the histogram in ImageJ (National Institutes of Health, http://rsb.info.nih.gov/ij). Signal levels were visualized by applying look-up tables (available on request). Signal colocalization was visualized as described (Sawchuk et al., 2008).

Chromatin immunoprecipitation

Chromatin immunoprecipitation was performed essentially as described (Jackson, 1978; Nagaki et al., 2003; Palma et al., 2007; Ponnusamy et al., 2008). Briefly, nuclei were isolated from ~2000 4-DAG seedlings (equivalent to ~2.5 g) per genotype per biological replicate, nuclear proteins were crosslinked to DNA with formaldehyde, chromatin was digested with micrococcal nuclease, and DNA-crosslinked fluorescent proteins were isolated using the μMACS GFP Isolation Kit (Miltenyi Biotec, Bergisch Gladbach, Germany). Enrichment of DNA of putative target regions in the *ATHB8* promoter was determined as described (Schubert et al., 2006) using a sequence of the *UBQ10* promoter to normalize results (Martin-Trillo et al., 2006). Details of primers are available upon request.

RESULTS

Vascular development in *Arabidopsis athb8* leaves

Null mutants of *ATHB8* display no obvious alterations in the vein patterns of mature leaves (Baima et al., 2001; Prigge et al., 2005). We first asked whether *ATHB8* could be assigned to any distinct function in vein formation or whether *ATHB8* activity is completely dispensable for this process. In *Arabidopsis*, veins of subsequent orders become recognizable progressively later in the same area of the developing leaf primordium, and veins of the same order appear in a tip-to-base sequence during leaf development (Candela et al., 1999; Kang and Dengler, 2002; Kang and Dengler, 2004; Kinsman and Pyke, 1998; Mattsson et al., 2003; Mattsson et al., 1999; Scarpella et al., 2004; Scarpella et al., 2006; Sieburth, 1999; Steynen and Schultz, 2003; Telfer and Poethig, 1994; Wenzel et al., 2007). Fig. 1A-D schematically depict the temporal sequence of vascular development events in *Arabidopsis* leaf primordia and define the stages and terminology to which we refer throughout this study.

Selection of ground cells that will acquire a preprocambial state, visualized through the dynamics of PIN1 expression (Scarpella et al., 2006; Wenzel et al., 2007), proceeded similarly in leaf primordia of wild type and of the null *athb8-11* mutant (see Fig. S1 in the supplementary material). However, we observed distinct anomalies in the assignment of the preprocambial cell state and procambial cell identity, marked by J1721:mGFP5er and Q0990:mGFP5er expression, respectively (Sawchuk et al., 2007), during *athb8-11* leaf development (for the attributes used to assess the representative nature of all displayed features and derived reproducibility quotients, see Table S1 in the supplementary material).

In wild type, J1721:mGFP5er expression is initiated in files of individual ground cells of the leaf primordium that coexpress *ATHB8* and that will successively elongate to acquire procambial cell identity (Sawchuk et al., 2007). Whereas at all stages of wild-type leaf development, J1721:mGFP5er expression was invariably constrained to narrow zones (Sawchuk et al., 2007) (Fig. 1E-H), newly emerged J1721:mGFP5er expression domains encompassed wide fields of cells in *athb8* leaf primordia (Fig. 1I-L). At later stages of vein development in *athb8* leaves, J1721:mGFP5er expression was, nevertheless, confined to strands of one or very few cell files (Fig. 1J-L).

In wild-type leaf development, Q0990:mGFP5er expression first emerges in files of elongated, *ATHB8*-expressing procambial cells, and all cells initiate Q0990:mGFP5er expression simultaneously throughout the length of a developing vein (Sawchuk et al., 2007). During unperturbed development, Q0990:mGFP5er expression is activated in a coordinated fashion in loop-forming lateral and marginal veins, such that expression appears simultaneously along entire vein loops (Sawchuk et al., 2007) (Fig. 1O,P). In *athb8* leaf development, however, Q0990:mGFP5er expression was switched on separately in lateral and marginal veins, and ectopic foci of transient epidermal expression were detected at the leaf margin during the development of the midvein and all loops (Fig. 1Q-T).

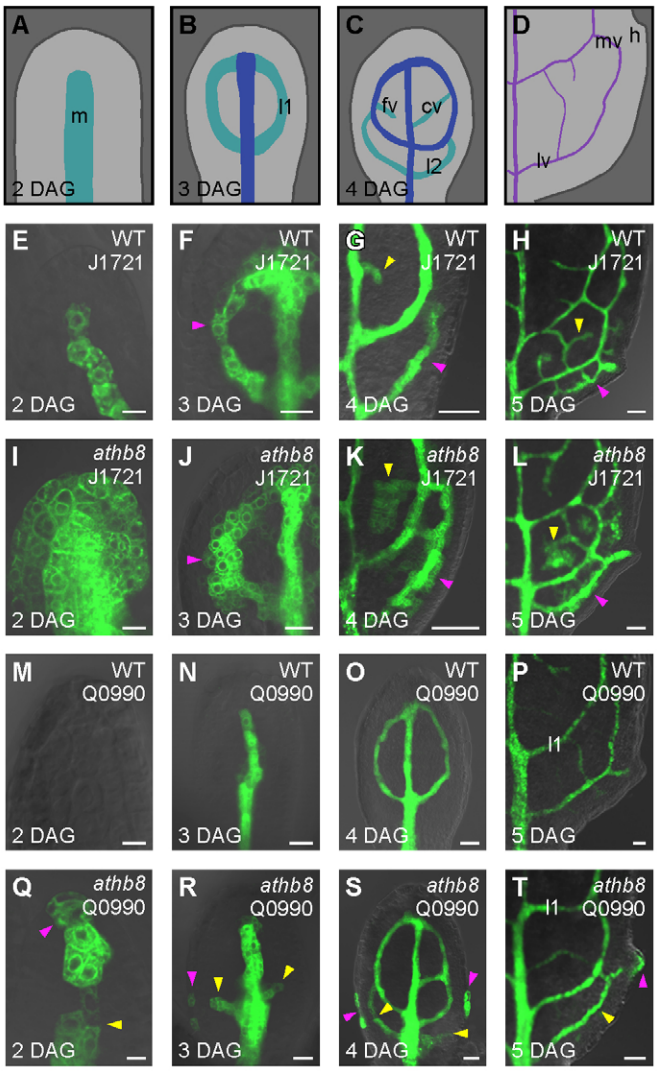

Fig. 1. Leaf vascular development in *Arabidopsis athb8*. (**A-T**) First leaf primordia, lateral (A,E,I,M,Q) or abaxial (B-D,F-H,J-L,N-P,R-T) view. Genotypes (WT, wild type) and markers are shown above, the age in days after germination (DAG) below. (A-D) Illustrations depicting the spatiotemporal course of vein formation in *Arabidopsis* first leaf development as inferred from published works (see text for references), and definition of terms used in this study. (A-C) Whole leaves. (D) Detail of the lower-right region of a mature leaf; note the smooth integration of lateral veins (lv) and marginal veins (mv) into vein loops. Cyan, preprocambial stages; blue, procambial stages; purple, mature veins; cv, connecting vein; fv, freely ending vein; h, hydathode; l1, first loop; l2; second loop; m, midvein. (E-T) Overlay of confocal laser microscopy and transmitted light images. (E-L) Preprocambium labeling by J1721:mGFP5er expression (green). Note the expanded expression domains in *athb8* leaves during formation of midvein (l), first, second and third loop (magenta arrowheads in J,K,L, respectively), and higher-order veins (yellow arrowheads in K,L); compare with wild type (E-H). (M-T) Procambium labeling by Q0990:mGFP5er expression (green). Note the epidermal foci of expression in *athb8* leaves during formation of midvein (magenta arrowhead in Q), first, second and third loop (magenta arrowheads in R,S,T, respectively). Furthermore, note the prematurely emerging expression domains marking development of midvein (yellow arrowhead in Q), first and second loop-forming lateral veins (yellow arrowheads in R,S, respectively), and entire second and third loops in *athb8* leaves (yellow arrowheads in S,T, respectively); compare with wild type (M-P). Scale bars: 5 μm in E,I,M,Q; 10 μm in F,J,N,R; 20 μm in G,H,K,L,O,P,S,T.

In summary, our results suggest that *ATHB8* is required to circumscribe preprocambial cell state assignment to narrow domains of ground cells and to integrate procambium identity acquisition within and between veins.

Auxin transport and response in *athb8* leaves

The appearance of expanded zones of J1721:mGFP5er expression and the asynchronous emergence of Q0990:mGFP5er expression domains observed during *athb8* leaf development are reminiscent of marker behavior under conditions of mild auxin transport inhibition (Sawchuk et al., 2007). Therefore, we next asked whether *athb8* leaves displayed altered sensitivity to the auxin transport inhibitor 1-N-naphthylphthalamic acid (NPA). Leaves of plants germinated and grown in the presence of auxin transport inhibitors are characterized by a number of distinct anomalies in vascular organization (Mattsson et al., 1999; Sieburth, 1999), most evident as great numbers of broad lateral veins and fusion of marginal veins to give rise to a continuous wide zone of vascular differentiation that extends along the entire margin of the leaf (Fig. 2C). Because these responses are quantifiable and NPA concentration dependent (Mattsson et al., 1999; Sieburth, 1999) (see Fig. S2 in the supplementary material), they can be used to assess sensitivity to auxin transport inhibition. At low concentrations of NPA, *athb8-11* leaves showed greater numbers of lateral veins, and a higher fraction of *athb8-11* leaves displayed the formation of a marginal vascular differentiation zone than wild-type leaves (Fig. 2A-D; see Fig. S2 in the supplementary material), suggesting that vein development in *athb8-11* is more susceptible to auxin transport inhibition. Similarly, leaves of the weaker *athb8-12* allele (Prigge et al., 2005) displayed hypersensitivity to NPA (see Fig. S2 in the supplementary material).

Wild-type leaves developing under conditions of reduced auxin transport display an expansion of PIN1 expression domains proportional to the level of auxin transport inhibition (Scarpella et al., 2006; Wenzel et al., 2007). We therefore asked whether the exaggerated response of vein patterns to auxin transport inhibition in *athb8* was associated with enhanced broadening of PIN1 expression fields under the same conditions. Concentrations of NPA that evoked a maximum differential response of vein patterns in *athb8* versus wild type resulted in higher levels and wider domains of $PIN1_{pro}$:PIN1:EYFP expression in *athb8-11* than in wild-type leaves (Fig. 2E-H). Because PIN1 expression in leaves is auxin inducible (Scarpella et al., 2006; Wenzel et al., 2007), we asked whether the exaggerated response of PIN1 expression to auxin transport inhibition in *athb8* could be attributable to abnormal auxin sensitivity. In leaves, the synthetic DR5 promoter (Ulmasov et al., 1997b) serves as a cell type-independent reporter of auxin response (Mattsson et al., 2003). Levels and patterns of $DR5Rev(9x)_{pro}$:ECFP-Nuc expression in *athb8-11* leaves, either under control conditions or upon treatment with exogenous auxin, were comparable to those in wild type (Fig. 2I-L).

We conclude that *ATHB8* is required for normal sensitivity of PIN1 expression and vascular patterns to auxin transport inhibition in the leaf, but that *ATHB8* appears expendable for leaf auxin response.

Expression of *ATHB8* in leaf development

In agreement with previous observations (Baima et al., 1995; Kang and Dengler, 2004; Sawchuk et al., 2007; Scarpella et al., 2004), we found that the 2.0 kb sequence upstream of the *ATHB8* translational start site is sufficient to drive expression of a nuclear-localized yellow fluorescent protein (HTA6:EYFP) (Zhang et al., 2005) in isodiametric cells of the leaf primordium that have been recruited

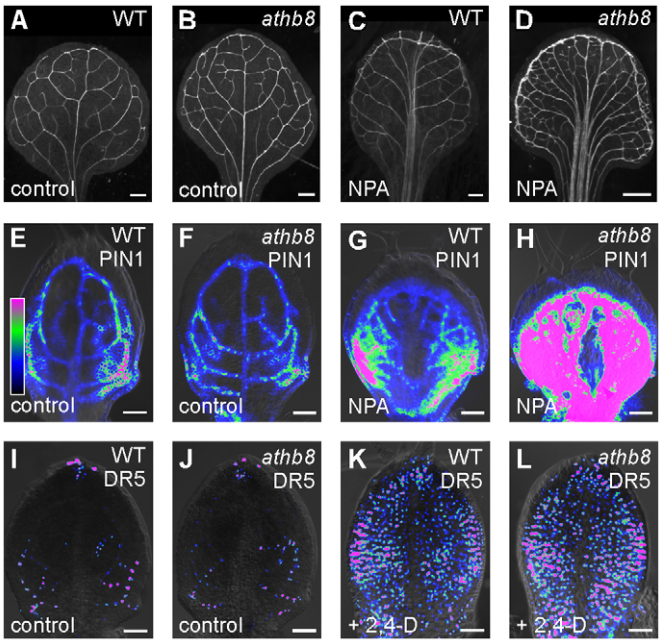

Fig. 2. Auxin transport and response in *athb8* leaves. (**A-L**) First leaves, abaxial view. Genotypes and markers are shown above, treatment (2.5 μM NPA or 10 μM 2,4-D) below. (A-D) Dark-field illumination of cleared mature leaves. (E-L) Overlay of confocal laser microscopy and transmitted light images. Images for each marker series were taken at an identical setting and are color-coded with an intensity LUT (as shown in E) in which black was used to encode background, and blue, green and magenta to encode increasing $PIN1_{pro}$::PIN1:EYFP (E-H) or $DR5Rev(9x)_{pro}$:ECFP-Nuc (I-L) signal levels. Scale bars: 0.5 mm in A-D; 25 μm in E-L.

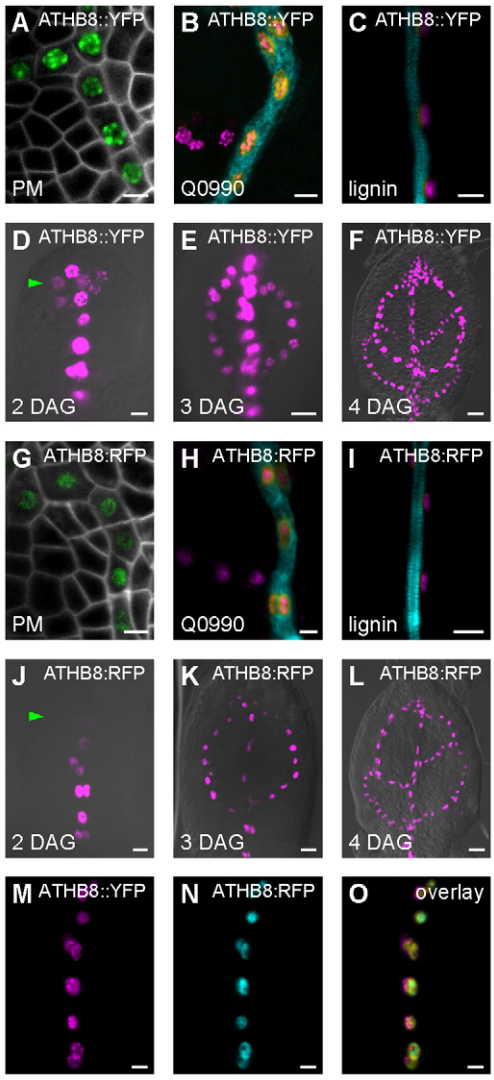

Fig. 3. *ATHB8* expression in leaf development. (**A-O**) First leaf primordia, abaxial (A-C,E-I,K-O) or lateral (D,J) view. Markers are shown above, age (DAG) (D-F,J-L) or additional markers (A-C,G-I) below. (A-C,G-I,M-O) Confocal laser microscopy images. (D-F,J-L) Overlay of confocal laser microscopy and transmitted light images. (A,G) Plasma membrane (PM) labeling by $UBQ10_{pro}$:EGFP:LTi6b expression (white). (A) $ATHB8_{pro}$:HTA6:EYFP expression (green). (B,H) Procambium labeling by Q0990:mGFP5er expression (cyan). (B-F,M,O) $ATHB8_{pro}$:HTA6:EYFP expression (magenta). (C,I) Xylem labeling by lignin autoflorescence (cyan). (G) $ATHB8_{pro}$:ATHB8:mCherry expression (green). (H-L) $ATHB8_{pro}$:ATHB8:mCherry expression (magenta). (J) Note the confined expression domain at the leaf tip (green arrowhead); compare with D. (N,O) $ATHB8_{pro}$:ATHB8:mCherry expression (cyan). (B,C,H,I,O) Images are color-coded with a dual-channel LUT from cyan to magenta through green, yellow and red (Demandolx and Davoust, 1997). Fluorescence in each detection channel was displayed in either magenta or cyan. Single-fluorophore images were then merged using a differential operator. As a result, a preponderance of cyan signal over colocalized magenta signal is encoded in green, opposite in red, and colocalized cyan and magenta signals of equal intensity in yellow. Scale bars: 5 μm in A,B,D,G,H,J,M-O; 10 μm in C,E,I,K; 20 μm in F,L.

towards Q0990:mGFP5er-labeled procambium formation (Fig. 3A,B) and that have therefore been designated as preprocambial cells (Mattsson et al., 2003). In leaf development, the intensity of $ATHB8_{pro}$:HTA6:EYFP signals was sustained in elongated procambial cells and eventually declined during late stages of vascular differentiation (Fig. 3B,C). As previously reported (Kang and Dengler, 2002; Scarpella et al., 2004), we additionally observed ephemeral activity of the *ATHB8* promoter at the leaf tip and hydathodes, where not all *ATHB8*-expressing cells will differentiate into vasculature (Fig. 3D; see Fig. S3 in the supplementary material).

Post-transcriptional regulation has been shown to spatially constrain fields of *ATHB8* expression in the root (Lee et al., 2006). To test whether post-transcriptional control impinges on domains of *ATHB8* expression in the leaf, we first visualized expression of a functional (see Materials and methods) translational fusion of *ATHB8* with the red fluorescent protein mCherry (Shaner et al., 2004) during leaf development. Expression of $ATHB8_{pro}$:ATHB8:mCherry was initiated in polygonal cells of the leaf primordium (Fig. 3G), maintained in elongated Q0990:mGFP5er-marked procambial cells (Fig. 3H), extinguished during terminal vascular differentiation (Fig. 3I), and was always absent at the leaf tip and hydathodes (Fig. 3J; see Fig. S3 in the supplementary material). Therefore, with the exception of the leaf tip and hydathode nonvascular areas, ATHB8:mCherry accumulation profiles are accurately recapitulated by *ATHB8* promoter-driven expression dynamics. We next asked whether imaging patterns of *ATHB8* promoter activity and tagged ATHB8 protein localization within the same sample could reveal subtle differences that would go unnoticed in comparative analyses performed on separate samples. Covisualization of $ATHB8_{pro}$:HTA6:EYFP and $ATHB8_{pro}$:ATHB8:mCherry signals

showed coincident expression of the two fluorescent proteins (Fig. 3M-O), suggesting that *ATHB8* promoter activity parallels ATHB8 protein expression in vascular cells and that post-transcriptional regulation does not revise vein-associated domains of *ATHB8* expression in the leaf.

Expression conferred by deletions of the *ATHB8* promoter

Because *ATHB8* expression is predicted by the activity of its upstream non-coding sequences, to identify regulatory elements required for preprocambial expression, we generated a series of *ATHB8* promoter variants. All the promoter fragments were fused to the nuclear-localized HTA6:EYFP in the context of the pFYTAG binary vector (Zhang et al., 2005). HTA6:EYFP driven by the cauliflower mosaic virus 35S –47 minimal promoter (Fang et al., 1989) was not able to generate detectable levels of YFP fluorescence in transgenic plants (see Fig. S4 in the supplementary material), suggesting that the T-DNA in the pFYTAG binary vector does not contain cryptic regulatory elements. Three criteria were sequentially adopted to test preprocambial expression of the promoter fragments: (1) stereotypical expression in leaves 4 days after germination (DAG), as inferred by comparison with expression directed by the 2.0 kb promoter fragment; (2) isodiametric shape of cells first expressing the promoter fragments, as determined by simultaneous visualization of ubiquitously expressed plasma membrane-localized GFP ($UBQ10_{pro}$:EGFP:LTi6b) (Sawchuk et al., 2008); (3) colocalization of the onset of expression with that of a nuclear-localized CFP driven by the 2.0 kb *ATHB8* promoter fragment ($ATHB8_{pro}$:ECFP-Nuc) (Sawchuk et al., 2007). Finally, vascular expression at stages later than preprocambial, as suggested by failure to satisfy criterion 1, was independently tested by simultaneous visualization of the procambial marker Q0990:mGFP5er (Sawchuk et al., 2007).

To initially demarcate the regulatory sequences that are required for *ATHB8* preprocambial expression, we generated a series of 0.5 kb 5′ deletions of the 2.0 kb *ATHB8* promoter (see Fig. S5 in the supplementary material). All deletions were designed so as not to interrupt putative cis-acting elements identified by available bioinformatics resources. The sequence of the *ATHB8* promoter between –964 and –1 was the shortest promoter fragment able to direct preprocambial expression (Fig. 4A-H), as the –501 to –1 fragment did not promote any leaf expression (Fig. 4I). This suggests that the 463 bp region of the *ATHB8* promoter between –964 and –501 is necessary for *ATHB8* preprocambial expression.

To test whether the *ATHB8* 5′ UTR in the –964 to –1 promoter fragment is essential to drive preprocambial expression, we deleted the sequence immediately downstream of the *ATHB8* transcriptional start site, as predicted by sequence alignment with the furthest upstream EST available (AV830211), while conserving a putative initiator sequence (Smale and Kadonaga, 2003) centered around the predicted transcription start site (see Fig. S5 in the supplementary material). The resulting 188 bp region of the *ATHB8* promoter between –964 and –776 was still able to impart preprocambial expression (Fig. 4J-L), suggesting that the *ATHB8* leader sequence is dispensable for preprocambial expression.

To further define the regulatory sequences required for *ATHB8* preprocambial expression, we generated a 5′ deletion of the –964 to –776 region at position –927 (see Fig. S5 in the supplementary material). The –927 to –1 promoter fragment was not able to drive vascular expression at preprocambial stages (Fig. 4M-P), suggesting that the 37 bp region of the *ATHB8* promoter from –964 to –927 is necessary for preprocambial expression.

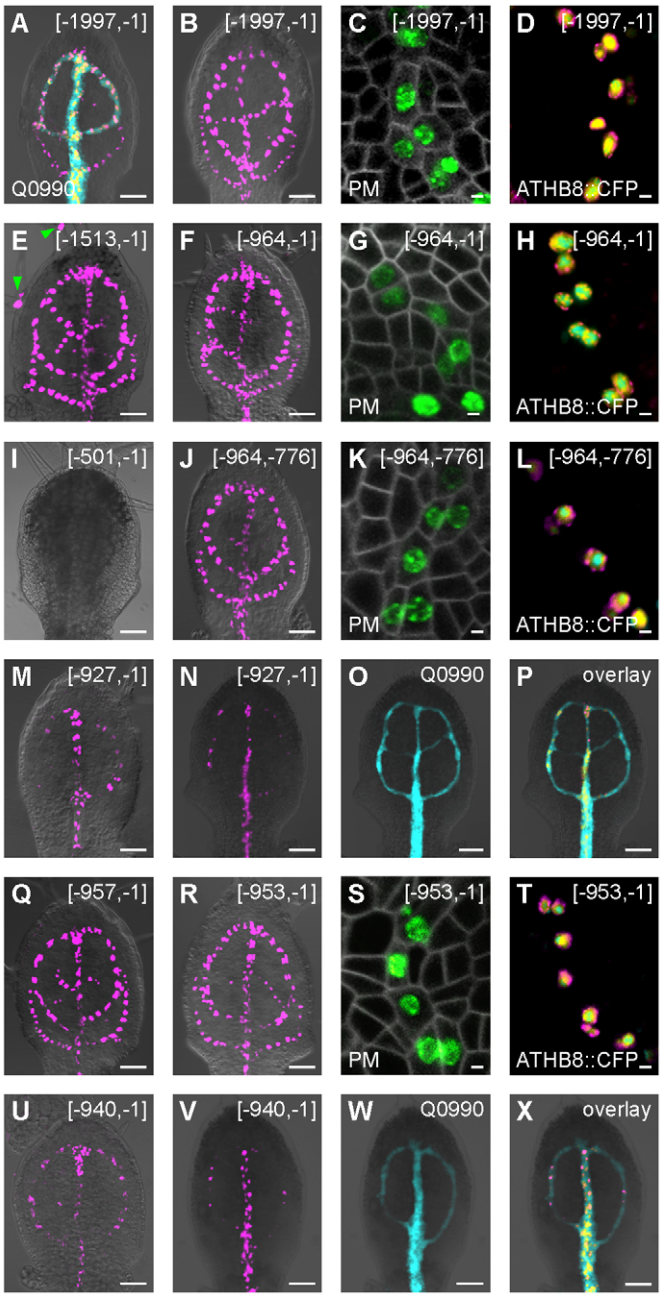

Fig. 4. Leaf expression conferred by *ATHB8* promoter deletions. (**A-X**) First leaves, abaxial view. Promoter variants (A-N,Q-V) or markers (O,P,W,X) are shown above, additional markers below. (A,B,E,F,I,J,M-R,U-X) Overlay of confocal laser microscopy and transmitted light images. (C,D,G,H,K,L,S,T) Confocal laser microscopy images. (A,D,H,L,P,T,X) Image color-coded with a dual-channel LUT as described for Fig. 3. (A,O,P,W,X) Procambium labeling by Q0990:mGFP5er expression (cyan). (A,B,D-F,H-J,L-N,P-R,T-V,X) HTA6:EYFP expression (magenta). (C,G,K,S) HTA6:EYFP expression (green) and plasma membrane (PM) labeling by $UBQ10_{pro}$:EGFP:LTi6b expression (white). (D,H,L,T) $ATHB8_{pro}$:ECFP-Nuc expression (cyan). (P,X) Overlay of images in N,O and V,W, respectively. (E) Note expression in trichomes (green arrowheads), which is absent with the –1997 to –1 and –964 to –1 promoter fragments, suggesting the presence of a suppressor of trichome expression in the –1997 to –1513 promoter region and the presence of an inducer of trichome expression in the –1513 to –964 promoter region. Scale bars: 25 μm in A,B,E,F,I,J,M-R,U-X; 2.5 μm in C,D,G,H,K,L,S,T.

Finally, to more precisely map the sequences essential for *ATHB8* preprocambial expression, we generated progressive 5′ deletions of the –964 to –927 region (see Fig. S5 in the supplementary material). Because the –940 to –1 promoter fragment was not able to direct vascular expression at preprocambial stages (Fig. 4U-X), the region from –953 to –1 constitutes the shortest fragment that still promoted preprocambial expression (Fig. 4R-T). This suggests that the 13 bp sequence between –953 and –940 of the *ATHB8* promoter is indispensable for *ATHB8* preprocambial expression.

Expression triggered by mutated variants of the *ATHB8* promoter

Interrogation of available databases of regulatory elements predicted the presence of core binding sites for MYB and GT1 transcription factors in the –953 to –940 *ATHB8* promoter fragment that is required for preprocambial expression (see Fig. S5 in the supplementary material). By manual inspection, we further identified a TGTCTG motif, which is a variant of the TGTCTC auxin-response element (ARE) (Li et al., 1994; Liu et al., 1994) (see Fig. S5 in the supplementary material). To test whether any of these putative regulatory elements are necessary for *ATHB8* preprocambial expression, we generated variants of the –953 to –1 *ATHB8* promoter fragment in which each of the three elements was individually mutated so as to abolish binding of the predicted transcription factor as previously determined experimentally (Gubler et al., 1999; Ouwerkerk et al., 1999; Ulmasov et al., 1997a; Ulmasov et al., 1997b) (see Fig. S5 in the supplementary material). As shown in Fig. 5, mutations in the MYB or GT1 presumed binding sites had no effect on the activity of the –953 to –1 *ATHB8* promoter fragment (Fig. 5A,C,D). However, mutation in the hypothetical ARE resulted in loss of expression at preprocambial stages (Fig. 5E-H). Furthermore, the expression induced by the –953 to –1 *ATHB8* promoter fragment containing the mutated TGTCTG element was indistinguishable from that induced by the –940 to –1 fragment, which deleted the entire region containing the MYB and GT1 core recognition sequences and the putative ARE (Fig. 5B,E). This suggests that the TGTCTG sequence in the –953 to –940 region of the *ATHB8* promoter is required for *ATHB8* preprocambial expression.

Auxin responsiveness of *ATHB8* promoter sequences

The TGTCTG element that we identified as being indispensable for *ATHB8* preprocambial expression is very similar to the TGTCTC element necessary for the auxin response (Li et al., 1994; Liu et al., 1994), and *ATHB8* expression is auxin inducible (Baima et al., 1995). To test whether *ATHB8* auxin responsiveness depends on the TGTCTG element and whether such a sequence therefore represents a functional ARE, we monitored patterns of HTA6:EYFP fluorescence conferred by *ATHB8* promoter variants in 4-DAG leaves after their exposure to the synthetic auxin 2,4-dichlorophenoxyacetic acid (2,4-D), comparing them to HTA6:EYFP expression in mock-treated samples. Auxin inducibility of the 2.0 kb *ATHB8* promoter (Fig. 6A,B) was largely retained by the –953 to –1 promoter fragment (Fig. 6C,D), suggesting that the region of the *ATHB8* promoter between –1997 and –953 does not contribute significantly to auxin-regulated *ATHB8* expression. Conversely, auxin responsiveness was lost in the –940 to –1 *ATHB8* promoter fragment (Fig. 6E,F), suggesting that the region of the *ATHB8* promoter between –953 and –940 is responsible for auxin inducibility. Within this region of the *ATHB8* promoter, mutation in the TGTCTG element, but not in the putative

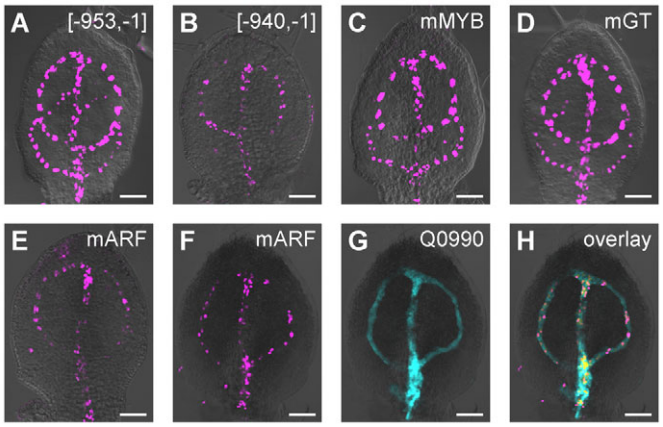

Fig. 5. Leaf expression conferred by mutated versions of the *ATHB8* promoter. (**A-H**) First leaves, abaxial view. Promoter variants are shown above. Overlay of confocal laser microscopy and transmitted light images. (A-F,H) HTA6:EYFP expression (magenta). (G,H) Procambium labeling by Q0990:mGFP5er expression (cyan). (H) Overlay of images in F,G. Image color-coded with a dual-channel LUT as described for Fig. 3. Scale bars: 25 μm.

MYB and GT1 binding sites, eliminated auxin responsiveness (Fig. 6G-L). Therefore, we conclude that the TGTCTG element in the *ATHB8* promoter is a functional ARE and that this sequence is required for both *ATHB8* preprocambial expression and auxin inducibility.

Regulators of *ATHB8* preprocambial expression

Transcription factors of the auxin-response factor (ARF) family have been shown to bind AREs in vitro (Guilfoyle and Hagen, 2001). Twenty-two ARFs have been identified in *Arabidopsis* (Guilfoyle and Hagen, 2007), and the TGTCTG element in the *ATHB8* promoter could be the target of several, if not all, of these ARFs (see below and Discussion). We focused on MONOPTEROS (MP; also known as ARF5) because of the reduced vascularization of *mp* leaves (Przemeck et al., 1996) and the decreased *ATHB8* transcript abundance in *mp* seedlings (Mattsson et al., 2003).

If MP is a regulator of *ATHB8* preprocambial expression, one would expect it to be at least partially coexpressed with *ATHB8*. To test this, we first monitored expression of a functional (see Materials and methods) translational fusion of *MP* with ECFP in leaf development. Unlike *ATHB8*, MP_{pro}:MP:ECFP expression was initiated in wide domains (Fig. 7A-C), but during leaf development these broad fields of expression resolved into narrower domains before subsiding to undetectable levels (Fig. 7B,C). To test whether MP expression domains represent locations of *ATHB8* expression, we visualized fluorescence in leaves simultaneously harboring $ATHB8_{pro}$:HTA6:EYFP and MP_{pro}:MP:ECFP, and invariantly observed overlap of $ATHB8_{pro}$:HTA6:EYFP signals with MP_{pro}:MP:ECFP expression (Fig. 7D).

If MP is a positive regulator of *ATHB8* expression at preprocambial stages, mutations in *MP* should at least reduce levels of *ATHB8* preprocambial expression. Expression of $ATHB8_{pro}$:HTA6:EYFP, and of HTA6:EYFP when driven by the –953 to –1 fragment of the *ATHB8* promoter, was initiated in preprocambial cells of wild-type leaves (Fig. 4A-D,R-T; Fig. 7E,F). However, the early stages of expression of these constructs were abolished in the background of the strong (see Materials and methods) *mp* mutant allele U55 (Fig. 5B,E-H; Fig. 7I,J).

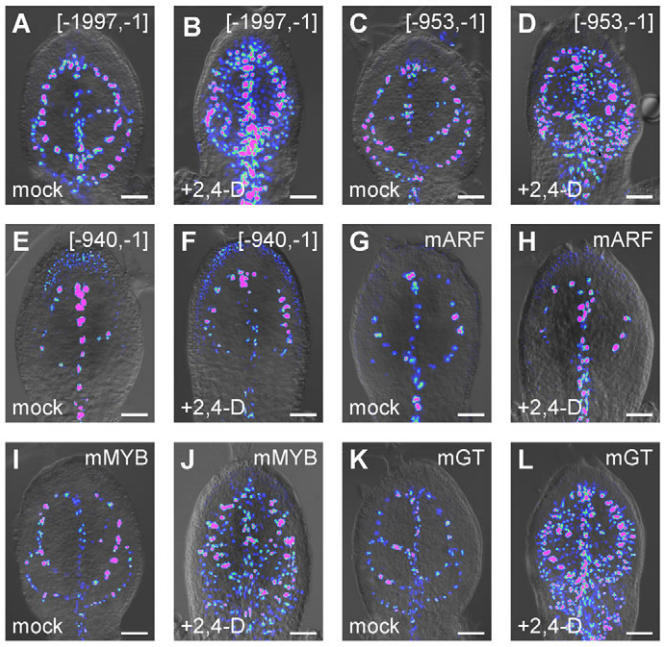

Fig. 6. Auxin responsiveness of *ATHB8* promoter sequences in the leaf. (**A-L**) First leaves, abaxial view. Promoter variants are shown above, treatment below. Overlay of confocal laser microscopy and transmitted light images. Images of mock and 2,4-D-treated leaves were taken at an identical setting and color-coded with an intensity LUT as described for Fig. 2. Scale bars: 25 µm.

Furthermore, their expression in *mp* leaves was remarkably similar to that conferred in wild type by loss or mutation of the TGTCTG element in the *ATHB8* promoter (Fig. 7G,H). Finally, expression of neither construct could be induced by exogenous 2,4-D in the *mp* mutant background (Fig. 7K,L). This suggests that MP is required for both *ATHB8* preprocambial expression and auxin inducibility, and that MP function at the *ATHB8* promoter is mediated by the TGTCTG element.

If MP activity is a limiting factor for *ATHB8* expression, ubiquitous MP expression should result in expansion of *ATHB8* expression domains. To test this, we visualized fields of ATHB8$_{pro}$:HTA6:EYFP activity in dexamethasone-exposed UBQ10$_{pro}$:MP:GR leaves and compared them with those in mock-treated leaves. Broadened ATHB8$_{pro}$:HTA6:EYFP expression domains were only detected in dexamethasone-treated samples (Fig. 7M,N), and this response was dependent on the presence of the TGTCTG element in the *ATHB8* promoter (Fig. 7O,P).

Finally, we asked whether MP directly regulates *ATHB8* expression. To test this, we immunoprecipitated chromatin-crosslinked ECFP in MP$_{pro}$:MP:ECFP and ATHB8$_{pro}$:ECFP-Nuc seedlings; we then assayed levels of co-precipitated *ATHB8* promoter regions in MP$_{pro}$:MP:ECFP and, to control for the binding of nuclear ECFP to the *ATHB8* promoter, in ATHB8$_{pro}$:ECFP-Nuc samples. We detected a statistically significant (P<0.001) 2.5-fold enrichment in the *ATHB8* promoter fragment that contains the TGTCTG element in MP$_{pro}$:MP:ECFP versus ATHB8$_{pro}$:ECFP-Nuc chromatin immunoprecipitates (Fig. 7Q), suggesting that MP resides in vivo at the *ATHB8* promoter.

In conclusion, our results suggest that the ARF MP is an essential, direct and positive regulator of *ATHB8* preprocambial expression and auxin responsiveness.

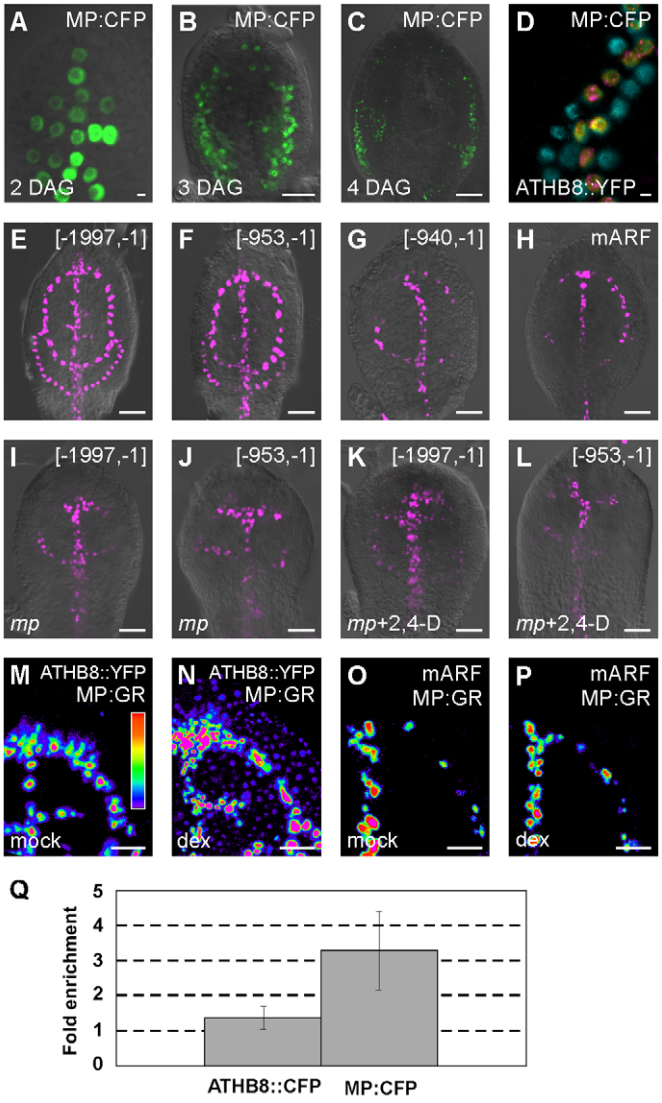

Fig. 7. Control of *ATHB8* leaf preprocambial expression. (**A-P**) First leaf primordia, lateral (A) or abaxial (B-P) view. Markers (A-D), promoter variants (E-P) and genotypes (M-P) are shown above, age (DAG) (A-C), additional markers (D), genotypes (I-L) and treatments (I-P) below. (A-C,E-L) Overlay of confocal laser microscopy and transmitted light images. (D,M-P) Confocal laser microscopy images. (A-C) MP$_{pro}$:MP:ECFP expression (green). (D) MP$_{pro}$:MP:ECFP expression (cyan). (D-L) HTA6:EYFP expression (magenta). (D) Image color-coded with a dual-channel LUT as described for Fig. 3. (M-P) Images of mock and dexamethasone-treated leaves were taken at an identical setting and color-coded with a spectral LUT (shown in M) in which black and magenta were used to encode zero-value and saturated pixels, respectively, and violet, blue, green, yellow, orange and red to encode increasing HTA6:EYFP signal levels. (**Q**) Enrichment of TGTCTG-containing *ATHB8* promoter fragments in chromatin immunoprecipitation assays performed on ATHB8$_{pro}$:ECFP-Nuc and MP$_{pro}$:MP:ECFP 4-DAG seedlings. Values indicate mean ± s.d. of three technical replicates for each of three (ATHB8$_{pro}$:ECFP-Nuc) or four (MP$_{pro}$:MP:ECFP) biological replicates. The difference between ATHB8$_{pro}$:ECFP-Nuc and MP$_{pro}$:MP:ECFP populations was analyzed with two-tailed unpaired *t*-test and was significant at P<0.001. For details, see Materials and methods. Scale bars: 2.5 µm in A,D; 25 µm in B,C,E-L; 10 µm in M-P.

Genetic interaction between *mp* and *athb8*

Recognizable effects of loss of *ATHB8* function in leaf vascular development are restricted to transient or conditional defects, but any additional regulatory potential of *ATHB8* might be masked by wild-type *MP* activity in *athb8* mutants. To test this, we compared vascular defects in mature leaves of the weak *mp* mutant allele *arf5-2* with those of the *arf5-2 athb8-11* double mutant. The *arf5-2* allele carries a single T-DNA insertion at the 3′ end of the *MP* coding region (see Materials and methods) and displayed ~40% penetrance of the rootless phenotype (85/871 seedlings segregating from *arf5-2* heterozygous parents). *arf5-2* homozygous seedlings could form an embryonic root and be grown on soil, but they were invariably sterile (44/44 *arf5-2* homozygous individuals found among 350 genotyped wild-type-looking plants segregating from *arf5-2* heterozygous parents). Most of the mature first leaves of rooted *arf5-2* seedlings (49/54) showed a vascular pattern complexity similar to that of wild-type or *athb8-11* first leaves (Fig. 8A,B,I). However, vein loops in *arf5-2* leaves were located further away from the leaf margin than in wild-type or *athb8-11* leaves ('centralized vasculature') (Fig. 8A,B,I). At maturity, approximately half of the first leaves of rootless *arf5-2* seedlings (32/69) were characterized by a normally complex, but centralized vein pattern, whereas the remaining half of the leaves displayed a simpler vascular organization (Fig. 8D,E,I). Finally, in ~60% of the leaves of either rooted or rootless *arf5-2* seedlings (32/54 and 41/69, respectively), the midvein bifurcated at the leaf tip (Fig. 8C,E,I). The overall complexity of vein pattern was only slightly reduced by additional loss of *ATHB8* function in the *arf5-2* background (Fig. 8I). However, ~80% of the leaves of either rooted (57/71) or rootless (35/46) *arf5-2 athb8-11* seedlings developed a terminally branched midvein (Fig. 8I), suggesting an enhancement of *arf5-2* leaf vascular defects in the double mutant, irrespective of its root phenotype.

If *ATHB8* preprocambial expression is contingent on any ARF activity additional to MP, the consequences of strongly reduced or complete loss of *MP* function on leaf vascular development should be further aggravated by additional deprivation of *ATHB8* activity. To test this, we compared patterns of vascularization in leaves of mp^{U55} with those of the mp^{U55} *athb8-11* double mutant. First leaves of the invariably rootless mp^{U55} seedlings displayed a dramatically simplified vascular organization, typically characterized by a bifurcated midvein and few additional vein fragments scattered across the lamina, and this phenotypic spectrum was not appreciably altered by supplemental loss of *ATHB8* function (Fig. 8I).

Like *athb8*, *mp* seedlings display enhanced sensitivity to auxin transport inhibition (Schuetz et al., 2008). Because loss of *ATHB8* function augments the effects of diminished *MP* activity on vein patterning, we asked whether the elevated response of *athb8* to auxin transport inhibitors could be further exacerbated in a background of reduced *MP* function. To test this, we assessed the sensitivity to NPA of single and double mutant combinations of *arf5-2* and *athb8-11*. Reduction in auxin transport frequently results in leaf fusion (Okada et al., 1991; Schuetz et al., 2008; Sieburth, 1999; Wang et al., 2005), a response that we first observed in wild type at 10 μM NPA (2/95) and in *athb8-11* at 5 μM NPA (2/33). Approximately 10% (3/29) of *arf5-2* seedlings displayed leaf fusion at 1 μM NPA, consistent with strong NPA hypersensitivity of *mp* mutants. At the same concentration of NPA, nearly 40% (10/27) of *arf5-2 athb8-11* double mutants displayed leaf fusion (Fig. 9H). Because loss of *ATHB8* function by itself did not result in leaf fusion at this concentration of NPA (Fig. 9F), we conclude that leaf separation defects elicited by reduced auxin transport in *arf5-2* are strongly enhanced by additional *athb8* mutation.

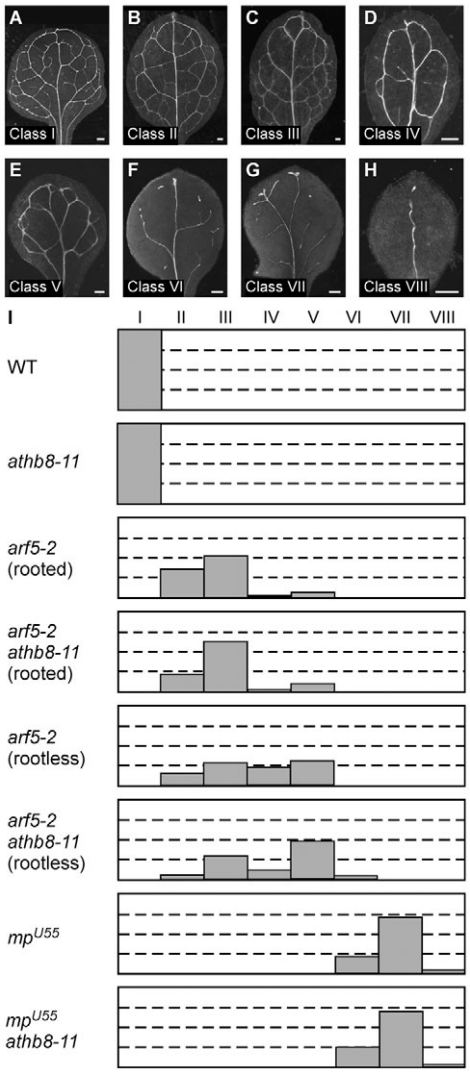

Fig. 8. Genetic interaction between *mp* and *athb8*. (**A-H**) Dark-field illumination of cleared mature leaves illustrating phenotypic classes: normal vasculature (A), centralized vasculature with unbranched midvein (B), centralized vasculature with bifurcated midvein (C), reduced vasculature with unbranched midvein (D), reduced vasculature with bifurcated midvein (E), fragmented vasculature with unbranched midvein (F), fragmented vasculature with bifurcated midvein (G), and solitary midvein (H). For details, see text. (**I**) Percentage of each phenotypic class in wild type, single mutants and double mutant combinations of *athb8-11* with weak (*arf5-2*) and strong (mp^{U55}) *mp* alleles. Dashed lines indicate 25, 50 and 75%. See also Table S2 in the supplementary material. Scale bars: 0.25 mm.

In summary, our results suggest that non-conditional and conditional contributions of *ATHB8* to leaf vascular patterning are covered by *MP* activity. Furthermore, our data suggest that any unique role of *ATHB8* in vein patterning becomes largely inconsequential upon severe loss of *MP* function and, therefore, that MP is the primary regulator of *ATHB8* non-redundant activities in leaf vascular patterning (see Discussion).

DISCUSSION

The molecular details of the mechanisms controlling the recruitment of ground cells in the leaf towards procambium formation are largely unknown. Substantial evidence has, however, been accumulating

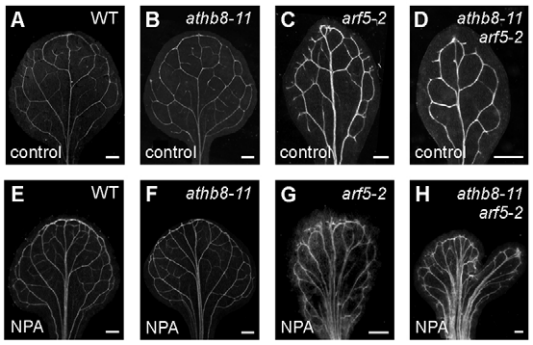

Fig. 9. Responsiveness of leaves of *mp* and *athb8* mutant combinations to auxin transport inhibition. (**A-H**) Dark-field illumination of cleared mature first leaves, abaxial view. Genotypes are shown above, treatments (1 μM NPA) below. See also Table S3 in the supplementary material. Scale bars: 0.5 mm.

that implicates polarly transported auxin signals in leaf vascular patterning (reviewed by Berleth et al., 2000; Sachs, 1981). Near-ubiquitous expression of the auxin exporter PIN1 narrows to files of procambial cells during leaf development (Scarpella et al., 2006; Wenzel et al., 2007), but how cells that will acquire procambial identity are selected among the population of PIN1-expressing cells is not known. Nevertheless, these anatomically inconspicuous 'preprocambial' cells can be identified by expression of the HD-Zip III gene *ATHB8*.

In this study, we have explored biological functions of *ATHB8* in leaf vascular development and searched for regulatory elements and trans-acting factors required for *ATHB8* preprocambial expression. We show that *ATHB8* is necessary to stabilize preprocambial cell specification against perturbations in auxin transport, to confine preprocambial cell state acquisition to narrow regions and to coordinate procambial cell identity assignment within and between veins. Further, we find that *ATHB8* expression in preprocambial cells depends on the presence of an ARE in its promoter. Finally, we show that the *ATHB8* preprocambial regulatory element is a direct target of the transcriptional regulator MP.

Non-redundant roles of *ATHB8* in leaf vascular development

Loss of *ATHB8* function leads to expanded expression of the preprocambial marker J1721 and asynchronous expression of the procambial marker Q0990. Expression of these reporters is strictly associated with zones of vascular differentiation in a variety of genetic backgrounds and under a number of experimental conditions (e.g. Dello Ioio et al., 2007; Leroy et al., 2007; Levesque et al., 2006; Sawchuk et al., 2007; Song et al., 2008; Weijers et al., 2005; Weijers et al., 2006), implicating *ATHB8* in constraining preprocambial state acquisition to narrow fields of cells and in coordinating procambial cell identity assignment within and between veins. Although premature differentiation of procambial strands in *athb8* leaves could simply represent a read-out of preprocambial defects, it is consistent with a proposed role for *ATHB8* in maintaining the meristematic potential of vascular cells (Baima et al., 2001; Kang and Dengler, 2002).

The behavior of J1721 and Q0990 in *athb8* strongly resembles that in wild type under conditions of reduced auxin transport (Sawchuk et al., 2007), suggesting a role for *ATHB8* in promoting auxin flow during early stages of vein formation. According to this interpretation, loss of *ATHB8* function would be expected to confer an enhanced response to auxin transport inhibitors. In the absence of alterations in auxin sensitivity, PIN1-labeled preprocambial cell specification and vein patterning are more sensitive to chemical obstruction of auxin flow in *athb8* than in wild type, suggesting the presence of auxin transport defects in the mutant. Alternatively, or additionally, the enhanced response of *athb8* leaves could suggest a function for *ATHB8* in stabilizing auxin flow against perturbations, consistent with the observed insensitivity of procambial strands to auxin transport inhibition (Mattsson et al., 1999).

Genetic or pharmacological interference with auxin flow generates broad areas of vascular differentiation (Mattsson et al., 1999; Sieburth, 1999), while it is difficult to explain, based on current knowledge, how exuberant preprocambial state acquisition and incongruent procambial identity assignment would per se result in hypersensitivity to auxin transport inhibition. Nevertheless, because of feedback between auxin flow and vascular development (Sachs, 1981), it is not currently possible to assign a fixed position to either of these processes in a linear cause-effect relationship. As such, the exaggerated response of *athb8* to auxin transport interference might underlie the altered marker behavior, or be a consequence of it, or the two might point to unrelated functions of *ATHB8* in vein formation. Although the assignment of a role for *ATHB8* in leaf vascular development at the molecular level will have to await the identification of its targets, the enhanced sensitivity of PIN1 expression and vascular patterns to obstruction of auxin flow in *athb8* leaves suggests that *ATHB8* is required to stabilize the selection of ground cells that will acquire a preprocambial state against perturbations in auxin transport.

Masked functions of *ATHB8* in vein patterning

Irregular vein formation in *athb8* leaves is corrected and eventually resolves into a normal leaf vascular pattern (Baima et al., 2001; Prigge et al., 2005). Amelioration of early vascular defects during organ development is not unprecedented (e.g. Scarpella et al., 2003), and responses of the vascular system to local auxin application or auxin transport inhibition are more severe when evaluated at early stages of vein development (Scarpella et al., 2006; Wenzel et al., 2007). How are defects at early stages of vein formation normalized during *athb8* leaf development? One possibility is that *ATHB8* has an ephemeral role that is confined to early stages of vascular strand formation and that it has an inconsequential function at later stages. Alternatively, or in addition, functional compensation among members of the HD-Zip III family could rectify defects due to loss of *ATHB8* activity.

If transience is an intrinsic property of the biological role of *ATHB8*, effects of loss of *ATHB8* function should not be expected to have long-lasting consequences in conditions of reduced activity of one of its regulators. The enhancement of vein pattern defects in *arf5-2 athb8-11* double mutants as compared with those in the weak *mp* allele *arf5-2* suggests, however, that *ATHB8* can have permanent effects on vein patterning. In leaves of *arf5-2*, the midvein frequently bifurcates at the leaf apex, a response that is commonly evoked by defective auxin transport (Mattsson et al., 1999; Sieburth, 1999). The fraction of leaves displaying this phenotype increases in the strong mp^{U55} allele, suggesting that the defect directly depends on *MP* function. In double-mutant combinations of *athb8-11* with *arf5-2*, no new phenotype class is observed; rather, the fraction of leaves displaying midvein bifurcation is increased to closely match that in the mp^{U55} allele. Strong *mp*/*arf5* alleles display an exaggerated response to auxin transport interference that results in obstruction of leaf formation (Schuetz et al., 2008), whereas enhanced sensitivity

to defective auxin flow in the weak *mp* allele *arf5-2* most conspicuously manifests in leaf fusion at very low concentrations of auxin transport inhibitors. Under these conditions, leaves of *athb8* mutants show normal sensitivity to auxin flow inhibition, but additional loss of *ATHB8* function greatly increases the occurrence of leaf separation defects in auxin transport-inhibited *arf5-2* seedlings. Therefore, *ATHB8* has functions in vein formation that extend beyond the evanescent contribution revealed by marker analysis and the moderate input exposed by auxin flow obstruction, but the regulatory potential of *ATHB8* is concealed in the *athb8* mutant background by the presence of functional *MP* activity.

If transience is not necessarily an inherent property of *ATHB8* function in leaf vascular development, then defects at early stages of vein formation in *athb8* could be amended at successive stages of development through the overlapping activities of other members of the HD-Zip III family, as shown for other aspects of plant development (Prigge et al., 2005). Because correction of *athb8* leaf vascular defects occurs to a lesser extent in the *arf5-2* background, one function of *MP* in vein development could be the regulation of the entire HD-Zip III family. Post-transcriptional downregulation of all members of the HD-Zip III family through overexpression of the microRNA 165 (*miR165*) results in cotyledon vascular defects that are remarkably similar to those displayed by strong *mp* alleles (Zhou et al., 2007), and expression of other members of the HD-Zip III family in addition to *ATHB8* is reduced in the *mp* background (Mattsson et al., 2003). If functional redundancy underlies amelioration of *athb8* vascular defects, the inability of the *athb8* mutation to shift the vein pattern complexity of *arf5-2* towards the severe distribution typical of mp^{U55} does not exclude a broader role for *ATHB8* in the regulation of leaf vascular patterning. However, further studies will be required to unravel the overlapping and redundant roles of HD-Zip III genes in vein formation.

Regulatory elements in preprocambial cell state acquisition

The *ATHB8* promoter is activated in files of ground cells that are stabilized towards the procambial fate (Kang and Dengler, 2004; Scarpella et al., 2004). Additionally, the *ATHB8* promoter induces transient expression at the tip of the leaf and at the hydathodes, where not all *ATHB8*-expressing cells will differentiate into vascular cells (Kang and Dengler, 2004; Scarpella et al., 2004). Expression of a functional *ATHB8* translational fusion recapitulates all aspects of *ATHB8* promoter activity with the exception of the nonvascular expression in the leaf tip and hydathode cells, suggesting the presence of post-transcriptional mechanisms that downregulate *ATHB8* expression at those locations. *ATHB8* transcripts are predicted to be targets of *miR165*-mediated degradation (Rhoades et al., 2002), and *miR165* is more abundantly expressed at the leaf tip (Li et al., 2005), suggesting that *miR165*-dependent post-transcriptional regulation of *ATHB8* expression might occur at locations of non-overlap between *ATHB8* promoter activity and expression of the *ATHB8* translational fusion.

Expression of *ATHB8* in preprocambial cells is strictly dependent on the presence of a TGTCTG element in its promoter. This element is a variant of the TGTCTC ARE (Li et al., 1994; Liu et al., 1994) and is required for auxin-induced *ATHB8* expression. That both preprocambial expression of *ATHB8* under unperturbed conditions and responsiveness of *ATHB8* to auxin signals are contingent on the activity of a single regulatory element is uncommon. In fact, the presence of a functional ARE in the promoter is not usually necessary for tissue- or stage-specific gene expression, only for a ubiquitous response to auxin signals (Li et al., 1994; Liu et al., 1994). Nevertheless, a synthetic promoter composed of repeats of the TGTCTC ARE coupled to a minimal viral promoter (DR5) (Ulmasov et al., 1997b) is sufficient to drive expression in developing veins (Mattsson et al., 2003). Furthermore, fields of DR5 promoter activity in leaf primordia seem to overlap with *ATHB8* preprocambial expression domains, although DR5 promoter-driven expression displays greater heterogeneity in onset, decay and level along individual veins (Mattsson et al., 2003; Scarpella et al., 2004). These observations suggest that in most auxin-responsive promoters, tissue-specific regulatory elements constrain the activity of AREs solely to auxin inducibility, whereas *ATHB8* preprocambial expression might be the unrestrained read-out of auxin signal transduction.

A confounding multitude of genes in *Arabidopsis* (~5000) contain a TGTCTG element in the 500 bp region immediately upstream of their coding sequence. This list includes genes expressed at early stages of vein development [e.g. *CYCA2;1* (Burssens et al., 2000), *SCL3* (Ckurshumova et al., 2009), *CESA2* (Beeckman et al., 2002)] and those with a proposed role in vascular development [e.g. *VAN3* (*SFC*) (Deyholos et al., 2000; Koizumi et al., 2000), *VAD1* (Lorrain et al., 2004), *VND4* (Kubo et al., 2005)] or auxin response [e.g. *ARF2* (Li et al., 2004), *AXR3* (*IAA17*) (Rouse et al., 1998), *HAT2* (Sawa et al., 2002)]. However, not all AREs present in promoters can bind ARFs in vitro (Inukai et al., 2005), and additional regulatory elements may constrain the regulatory potential of AREs to sole auxin responsiveness (Li et al., 1994; Liu et al., 1994). Therefore, we consider it unlikely that all these genes are expressed in preprocambial cells. If the presence of a TGTCTG element in the promoter is unlikely to be sufficient to predict expression in preprocambial cells, what other requirements are necessary for preprocambial expression? Nucleotides flanking the TGTCTC ARE seem to act as modifiers of ARE activity (Ulmasov et al., 1997a; Ulmasov et al., 1995; Ulmasov et al., 1997b). Vast systematic efforts will be necessary to test in vivo what, if any, boundary conditions are required for TGTC-containing elements to promote preprocambial expression.

Regulation of preprocambial cell state acquisition by ARF proteins

Transcription factors of the ARF family have been shown to bind AREs in vitro (reviewed by Guilfoyle and Hagen, 2001). Deletion or mutation of the TGTCTG ARE in the *ATHB8* promoter eliminates preprocambial expression but does not induce expression in nonvascular cells. This observation suggests that the TGTCTG element is not the target of a repressor that normally extinguishes *ATHB8* expression outside of the vasculature, but rather that an activator binds the TGTCTG element and induces *ATHB8* expression in vascular cells. In *Arabidopsis*, the ARF family is encoded by 22 genes, of which five [*MP* (*ARF5*), *ARF6*, *ARF7* (*NPH4*), *ARF8* and *ARF19*] function as transcriptional activators in transfected protoplasts, whereas the remaining 17 behave as repressors in a similar experimental context (Guilfoyle and Hagen, 2007) (and references therein). *ATHB8* preprocambial expression is under the direct control of MP, which is consistent with reduced *ATHB8* transcript levels in an *mp* background (Mattsson et al., 2003). None of these observations, however, excludes the involvement of other ARFs in the control of *ATHB8* preprocambial expression. At least three of the four remaining activating ARFs are expressed in domains that may overlap with those of *ATHB8* (Hardtke et al., 2004; Li et al., 2006; Okushima et al., 2005; Tian et al., 2004; Wilmoth et al., 2005), and the class of activating ARFs is characterized by a high level of functional redundancy among its members (Hardtke et al., 2004; Nagpal et al., 2005; Okushima et al., 2005; Wilmoth et al., 2005). Further, because the tests for activation

and repression of transcription by members of the ARF family rely upon transient expression assays in leaf mesophyll or suspension cell culture protoplasts, it remains possible that an ARF classified as a repressor could function as an activator, and vice versa, in certain cell types or environments (e.g. Okushima et al., 2005). Conditional manipulation of gene activity will be required to expose the overlapping and non-redundant roles of ARFs in the regulation of *ATHB8* preprocambial expression, as any further reduction of ARF activity than that residual in strong *mp* backgrounds is likely to directly impinge on leaf primordium formation (Hardtke et al., 2004). However, deletion or mutation of the TGTCTG element in the *ATHB8* promoter confers expression in wild type that is indistinguishable from that of the full-length *ATHB8* promoter in the strong mp^{U55} allele. Moreover, leaf vascular defects in mp^{U55} cannot be further enhanced by additional loss of *ATHB8* function. Therefore, the contribution of ARFs other than MP to the control of *ATHB8* preprocambial expression is probably subtle.

A functional *MP* translational fusion is at first detected in nearly all subepidermal cells of the young leaf primordium, and its expression is only subsequently confined to sites of vein formation. This is strikingly different from the activity of the *ATHB8* promoter, which is initiated in single cell files before expression of the MP fusion protein has been restricted to the narrow sites of vein formation. Further, ubiquitous *MP* expression results in expanded domains of *ATHB8* expression, which do not, however, extend to include all cells in the leaf. Although it will be interesting in the future to understand how broad patterns of *MP* expression are translated into narrow sites of *ATHB8* activation, the identification of regulators of early vein development and of the transcription factors controlling their expression already assists in defining the contribution of auxin signal transduction to leaf vascular patterning at the molecular level.

Acknowledgements

We thank Ben Nilsson for crosses; the *Arabidopsis* Biological Resource Center, Thomas Berleth, Robert Campbell, Taku Demura, David Galbraith, Jim Mattsson, Ben Scheres, Mathias Schuetz, Roger Tsien and Jian Xu for kindly providing seeds and plasmids; Dolf Weijers for generously sharing unpublished material and results; and Thomas Berleth for inspiring discussions and critical reading of the manuscript. This work was supported by a Discovery Grant of the Natural Sciences and Engineering Research Council of Canada (NSERC), by an Alberta Ingenuity (AI) New Faculty Grant and by the Canada Research Chairs Program. T.J.D. was supported by an NSERC CGS-M Scholarship and an AI Student Scholarship.

Supplementary material

Supplementary material for this article is available at
http://dev.biologists.org/cgi/content/full/136/19/3235/DC1

References

Alonso-Peral, M. M., Candela, H., del Pozo, J. C., Martinez-Laborda, A., Ponce, M. R. and Micol, J. L. (2006). The HVE/CAND1 gene is required for the early patterning of leaf venation in Arabidopsis. *Development* **133**, 3755-3766.

Baima, S., Nobili, F., Sessa, G., Lucchetti, S., Ruberti, I. and Morelli, G. (1995). The expression of the Athb-8 homeobox gene is restricted to provascular cells in Arabidopsis thaliana. *Development* **121**, 4171-4182.

Baima, S., Possenti, M., Matteucci, A., Wisman, E., Altamura, M. M., Ruberti, I. and Morelli, G. (2001). The Arabidopsis ATHB-8 HD-zip protein acts as a differentiation-promoting transcription factor of the vascular meristems. *Plant Physiol.* **126**, 643-655.

Beeckman, T., Przemeck, G. K., Stamatiou, G., Lau, R., Terryn, N., De Rycke, R., Inze, D. and Berleth, T. (2002). Genetic complexity of cellulose synthase a gene function in Arabidopsis embryogenesis. *Plant Physiol.* **130**, 1883-1893.

Berleth, T. and Jurgens, G. (1993). The role of the monopteros gene in organizing the basal body region of the Arabidopsis embryo. *Development* **118**, 575-587.

Berleth, T., Mattsson, J. and Hardtke, C. S. (2000). Vascular continuity and auxin signals. *Trends Plant Sci.* **5**, 387-393.

Burssens, S., de Almeida Engler, J., Beeckman, T., Richard, C., Shaul, O., Ferreira, P., Van Montagu, M. and Inze, D. (2000). Developmental expression of the Arabidopsis thaliana CycA2;1 gene. *Planta* **211**, 623-631.

Candela, H., Martinez-Laborda, A. and Micol, J. L. (1999). Venation pattern formation in Arabidopsis thaliana vegetative leaves. *Dev. Biol.* **205**, 205-216.

Carland, F. M. and Nelson, T. (2004). Cotyledon vascular pattern2-mediated inositol (1,4,5) triphosphate signal transduction is essential for closed venation patterns of Arabidopsis foliar organs. *Plant Cell* **16**, 1263-1275.

Ckurshumova, W., Koizumi, K., Chatfield, S. P., Sanchez-Buelna, S. U., Gangaeva, A. E., McKenzie, R. and Berleth, T. (2009). Tissue-specific GAL4 expression patterns as a resource enabling targeted gene expression, cell type-specific transcript profiling and gene function characterization in the Arabidopsis vascular system. *Plant Cell Physiol.* **50**, 141-150.

Cnops, G., Neyt, P., Raes, J., Petrarulo, M., Nelissen, H., Malenica, N., Luschnig, C., Tietz, O., Ditengou, F., Palme, K. et al. (2006). The TORNADO1 and TORNADO2 genes function in several patterning processes during early leaf development in Arabidopsis thaliana. *Plant Cell* **18**, 852-866.

Dello Ioio, R., Linhares, F. S., Scacchi, E., Casamitjana-Martinez, E., Heidstra, R., Costantino, P. and Sabatini, S. (2007). Cytokinins determine Arabidopsis root-meristem size by controlling cell differentiation. *Curr. Biol.* **17**, 678-682.

Demandolx, D. and Davoust, J. (1997). Multicolour analysis and local image correlation in confocal microscopy. *J. Micros.* **185**, 21-36.

Deyholos, M. K., Cordner, G., Beebe, D. and Sieburth, L. E. (2000). The SCARFACE gene is required for cotyledon and leaf vein patterning. *Development* **127**, 3205-3213.

Esau, K. (1943). Origin and development of primary vascular tissues in plants. *Bot. Rev.* **9**, 125-206.

Esau, K. (1965). *Plant Anatomy*. New York: John Wiley.

Fang, R. X., Nagy, F., Sivasubramaniam, S. and Chua, N. H. (1989). Multiple cis regulatory elements for maximal expression of the cauliflower mosaic virus 35S promoter in transgenic plants. *Plant Cell* **1**, 141-150.

Foster, A. S. (1952). Foliar venation in angiosperms from an ontogenetic standpoint. *Am. J. Bot.* **39**, 752-766.

Gubler, F., Raventos, D., Keys, M., Watts, R., Mundy, J. and Jacobsen, J. V. (1999). Target genes and regulatory domains of the GAMYB transcriptional activator in cereal aleurone. *Plant J.* **17**, 1-9.

Guilfoyle, T. J. and Hagen, G. (2001). Auxin response factors. *J. Plant Growth Regul.* **20**, 281-291.

Guilfoyle, T. J. and Hagen, G. (2007). Auxin response factors. *Curr. Opin. Plant Biol.* **10**, 453-460.

Hardtke, C. S. and Berleth, T. (1998). The Arabidopsis gene MONOPTEROS encodes a transcription factor mediating embryo axis formation and vascular development. *EMBO J.* **17**, 1405-1411.

Hardtke, C. S., Ckurshumova, W., Vidaurre, D. P., Singh, S. A., Stamatiou, G., Tiwari, S. B., Hagen, G., Guilfoyle, T. J. and Berleth, T. (2004). Overlapping and non-redundant functions of the Arabidopsis auxin response factors MONOPTEROS and NONPHOTOTROPIC HYPOCOTYL 4. *Development* **131**, 1089-1100.

Inukai, Y., Sakamoto, T., Ueguchi-Tanaka, M., Shibata, Y., Gomi, K., Umemura, I., Hasegawa, Y., Ashikari, M., Kitano, H. and Matsuoka, M. (2005). Crown rootless1, which is essential for crown root formation in rice, is a target of an AUXIN RESPONSE FACTOR in auxin signaling. *Plant Cell* **17**, 1387-1396.

Jackson, V. (1978). Studies on histone organization in the nucleosome using formaldehyde as a reversible cross-linking agent. *Cell* **15**, 945-954.

Kang, J. and Dengler, N. (2002). Cell cycling frequency and expression of the homeobox gene ATHB-8 during leaf vein development in Arabidopsis. *Planta* **216**, 212-219.

Kang, J. and Dengler, N. (2004). Vein pattern development in adult leaves of Arabidopsis thaliana. *Int. J. Plant Sci.* **165**, 231-242.

Kinsman, E. A. and Pyke, K. A. (1998). Bundle sheath cells and cell-specific plastid development in Arabidopsis leaves. *Development* **125**, 1815-1822.

Koizumi, K., Sugiyama, M. and Fukuda, H. (2000). A series of novel mutants of Arabidopsis thaliana that are defective in the formation of continuous vascular network: calling the auxin signal flow canalization hypothesis into question. *Development* **127**, 3197-3204.

Kubo, M., Udagawa, M., Nishikubo, N., Horiguchi, G., Yamaguchi, M., Ito, J., Mimura, T., Fukuda, H. and Demura, T. (2005). Transcription switches for protoxylem and metaxylem vessel formation. *Genes Dev.* **19**, 1855-1860.

Lee, J. Y., Colinas, J., Wang, J. Y., Mace, D., Ohler, U. and Benfey, P. N. (2006). Transcriptional and posttranscriptional regulation of transcription factor expression in Arabidopsis roots. *Proc. Natl. Acad. Sci. USA* **103**, 6055-6060.

Leroy, O., Hennig, L., Breuninger, H., Laux, T. and Kohler, C. (2007). Polycomb group proteins function in the female gametophyte to determine seed development in plants. *Development* **134**, 3639-3648.

Levesque, M. P., Vernoux, T., Busch, W., Cui, H. C., Wang, J. Y., Blilou, I., Hassan, H., Nakajima, K., Matsumoto, N., Lohmann, J. U. et al. (2006). Whole-genome analysis of the SHORT-ROOT developmental pathway in Arabidopsis. *PLoS Biol.* **4**, 739-752.

Li, H., Johnson, P., Stepanova, A., Alonso, J. M. and Ecker, J. R. (2004). Convergence of signaling pathways in the control of differential cell growth in Arabidopsis. *Dev. Cell* **7**, 193-204.
Li, H., Xu, L., Wang, H., Yuan, Z., Cao, X., Yang, Z., Zhang, D., Xu, Y. and Huang, H. (2005). The Putative RNA-dependent RNA polymerase RDR6 acts synergistically with ASYMMETRIC LEAVES1 and 2 to repress BREVIPEDICELLUS and MicroRNA165/166 in Arabidopsis leaf development. *Plant Cell* **17**, 2157-2171.
Li, J., Dai, X. and Zhao, Y. (2006). A role for auxin response factor 19 in auxin and ethylene signaling in Arabidopsis. *Plant Physiol.* **140**, 899-908.
Li, Y., Liu, Z. B., Shi, X., Hagen, G. and Guilfoyle, T. J. (1994). An auxin-inducible element in soybean SAUR promoters. *Plant Physiol.* **106**, 37-43.
Liu, Z. B., Ulmasov, T., Shi, X., Hagen, G. and Guilfoyle, T. J. (1994). Soybean GH3 promoter contains multiple auxin-inducible elements. *Plant Cell* **6**, 645-657.
Lorrain, S., Lin, B., Auriac, M. C., Kroj, T., Saindrenan, P., Nicole, M., Balague, C. and Roby, D. (2004). Vascular associated death1, a novel GRAM domain-containing protein, is a regulator of cell death and defense responses in vascular tissues. *Plant Cell* **16**, 2217-2232.
Martin-Trillo, M., Lazaro, A., Poethig, R. S., Gomez-Mena, C., Pineiro, M. A., Martinez-Zapater, J. M. and Jarillo, J. A. (2006). EARLY IN SHORT DAYS 1 (ESD1) encodes ACTIN-RELATED PROTEIN 6 (AtARP6), a putative component of chromatin remodelling complexes that positively regulates FLC accumulation in Arabidopsis. *Development* **133**, 1241-1252.
Mattsson, J., Sung, Z. R. and Berleth, T. (1999). Responses of plant vascular systems to auxin transport inhibition. *Development* **126**, 2979-2991.
Mattsson, J., Ckurshumova, W. and Berleth, T. (2003). Auxin signaling in Arabidopsis leaf vascular development. *Plant Physiol.* **131**, 1327-1339.
Nagaki, K., Talbert, P. B., Zhong, C. X., Dawe, R. K., Henikoff, S. and Jiang, J. (2003). Chromatin immunoprecipitation reveals that the 180-bp satellite repeat is the key functional DNA element of Arabidopsis thaliana centromeres. *Genetics* **163**, 1221-1225.
Nagpal, P., Ellis, C. M., Weber, H., Ploense, S. E., Barkawi, L. S., Guilfoyle, T. J., Hagen, G., Alonso, J. M., Cohen, J. D., Farmer, E. E. et al. (2005). Auxin response factors ARF6 and ARF8 promote jasmonic acid production and flower maturation. *Development* **132**, 4107-4118.
Nelson, T. and Dengler, N. (1997). Leaf vascular pattern formation. *Plant Cell* **9**, 1121-1135.
Okada, K., Ueda, J., Komaki, M. K., Bell, C. J. and Shimura, Y. (1991). Requirement of the auxin polar transport system in early stages of Arabidopsis floral bud formation. *Plant Cell* **3**, 677-684.
Okushima, Y., Overvoorde, P. J., Arima, K., Alonso, J. M., Chan, A., Chang, C., Ecker, J. R., Hughes, B., Lui, A., Nguyen, D. et al. (2005). Functional genomic analysis of the AUXIN RESPONSE FACTOR gene family members in Arabidopsis thaliana: unique and overlapping functions of ARF7 and ARF19. *Plant Cell* **17**, 444-463.
Ouwerkerk, P. B., Trimborn, T. O., Hilliou, F. and Memelink, J. (1999). Nuclear factors GT-1 and 3AF1 interact with multiple sequences within the promoter of the Tdc gene from Madagascar periwinkle: GT-1 is involved in UV light-induced expression. *Mol. Gen. Genet.* **261**, 610-622.
Palma, K., Zhao, Q., Cheng, Y. T., Bi, D., Monaghan, J., Cheng, W., Zhang, Y. and Li, X. (2007). Regulation of plant innate immunity by three proteins in a complex conserved across the plant and animal kingdoms. *Genes Dev.* **21**, 1484-1493.
Petricka, J. J. and Nelson, T. M. (2007). Arabidopsis nucleolin affects plant development and patterning. *Plant Physiol.* **144**, 173-186.
Pineau, C., Freydier, A., Ranocha, P., Jauneau, A., Turner, S., Lemonnier, G., Renou, J. P., Tarkowski, P., Sandberg, G., Jouanin, L. et al. (2005). hca: an Arabidopsis mutant exhibiting unusual cambial activity and altered vascular patterning. *Plant J.* **44**, 271-289.
Ponnusamy, S., Alderson, N. L., Hama, H., Bielawski, J., Jiang, J. C., Bhandari, R., Snyder, S. H., Jazwinski, S. M. and Ogretmen, B. (2008). Regulation of telomere length by fatty acid elongase 3 in yeast. Involvement of inositol phosphate metabolism and Ku70/80 function. *J. Biol. Chem.* **283**, 27514-27524.
Pray, T. R. (1955). Foliar venation in Angiosperms. II. Histogenesis of the venation of Liriodendron. *Am. J. Bot.* **42**, 18-27.
Prigge, M. J., Otsuga, D., Alonso, J. M., Ecker, J. R., Drews, G. N. and Clark, S. E. (2005). Class III homeodomain-leucine zipper gene family members have overlapping, antagonistic, and distinct roles in Arabidopsis development. *Plant Cell* **17**, 61-76.
Przemeck, G. K., Mattsson, J., Hardtke, C. S., Sung, Z. R. and Berleth, T. (1996). Studies on the role of the Arabidopsis gene MONOPTEROS in vascular development and plant cell axialization. *Planta* **200**, 229-237.
Rhoades, M. W., Reinhart, B. J., Lim, L. P., Burge, C. B., Bartel, B. and Bartel, D. P. (2002). Prediction of plant microRNA targets. *Cell* **110**, 513-520.
Rouse, D., Mackay, P., Stirnberg, P., Estelle, M. and Leyser, O. (1998). Changes in auxin response from mutations in an AUX/IAA gene. *Science* **279**, 1371-1373.
Sablowski, R. W. and Meyerowitz, E. M. (1998). A homolog of NO APICAL MERISTEM is an immediate target of the floral homeotic genes APETALA3/PISTILLATA. *Cell* **92**, 93-103.
Sachs, T. (1981). The control of the patterned differentiation of vascular tissues. *Adv. Bot. Res.* **9**, 151-262.
Sachs, T. (1989). The development of vascular networks during leaf development. *Curr. Top. Plant Biochem. Physiol.* **8**, 168-183.
Sawa, S., Ohgishi, M., Goda, H., Higuchi, K., Shimada, Y., Yoshida, S. and Koshiba, T. (2002). The HAT2 gene, a member of the HD-Zip gene family, isolated as an auxin inducible gene by DNA microarray screening, affects auxin response in Arabidopsis. *Plant J.* **32**, 1011-1022.
Sawchuk, M. G., Head, P., Donner, T. J. and Scarpella, E. (2007). Time-lapse imaging of Arabidopsis leaf development shows dynamic patterns of procambium formation. *New Phytol.* **176**, 560-571.
Sawchuk, M. G., Donner, T. J., Head, P. and Scarpella, E. (2008). Unique and overlapping expression patterns among members of photosynthesis-associated nuclear gene families in Arabidopsis. *Plant Physiol.* **148**, 1908-1924.
Scarpella, E., Rueb, S. and Meijer, A. H. (2003). The RADICLELESS1 gene is required for vascular pattern formation in rice. *Development* **130**, 645-658.
Scarpella, E., Francis, P. and Berleth, T. (2004). Stage-specific markers define early steps of procambium development in Arabidopsis leaves and correlate termination of vein formation with mesophyll differentiation. *Development* **131**, 3445-3455.
Scarpella, E., Marcos, D., Friml, J. and Berleth, T. (2006). Control of leaf vascular patterning by polar auxin transport. *Genes Dev.* **20**, 1015-1027.
Schubert, D., Primavesi, L., Bishopp, A., Roberts, G., Doonan, J., Jenuwein, T. and Goodrich, J. (2006). Silencing by plant Polycomb-group genes requires dispersed trimethylation of histone H3 at lysine 27. *EMBO J.* **25**, 4638-4649.
Schuetz, M., Berleth, T. and Mattsson, J. (2008). Multiple MONOPTEROS-dependent pathways are involved in leaf initiation. *Plant Physiol.* **148**, 870-880.
Shaner, N. C., Campbell, R. E., Steinbach, P. A., Giepmans, B. N., Palmer, A. E. and Tsien, R. Y. (2004). Improved monomeric red, orange and yellow fluorescent proteins derived from Discosoma sp. red fluorescent protein. *Nat. Biotechnol.* **22**, 1567-1572.
Sieburth, L. E. (1999). Auxin is required for leaf vein pattern in Arabidopsis. *Plant Physiol.* **121**, 1179-1190.
Smale, S. T. and Kadonaga, J. T. (2003). The RNA polymerase II core promoter. *Annu. Rev. Biochem.* **72**, 449-479.
Song, S. K., Hofhuis, H., Lee, M. M. and Clark, S. E. (2008). Key divisions in the early Arabidopsis embryo require POL and PLL1 Phosphatases to establish the root stem cell organizer and vascular axis. *Dev. Cell* **15**, 98-109.
Steynen, Q. J. and Schultz, E. A. (2003). The FORKED genes are essential for distal vein meeting in Arabidopsis. *Development* **130**, 4695-4708.
Telfer, A. and Poethig, R. S. (1994). Leaf development in Arabidopsis. In *Arabidopsis* (ed. E. M. Meyerowitz and C. R. Somerville), pp. 379-401. Cold Spring Harbor, NY: Cold Spring Harbor Laboratory Press.
Tian, C. E., Muto, H., Higuchi, K., Matamura, T., Tatematsu, K., Koshiba, T. and Yamamoto, K. T. (2004). Disruption and overexpression of auxin response factor 8 gene of Arabidopsis affect hypocotyl elongation and root growth habit, indicating its possible involvement in auxin homeostasis in light condition. *Plant J.* **40**, 333-343.
Ulmasov, T., Liu, Z. B., Hagen, G. and Guilfoyle, T. J. (1995). Composite structure of auxin response elements. *Plant Cell* **7**, 1611-1623.
Ulmasov, T., Hagen, G. and Guilfoyle, T. J. (1997a). ARF1, a transcription factor that binds to auxin response elements. *Science* **276**, 1865-1868.
Ulmasov, T., Murfett, J., Hagen, G. and Guilfoyle, T. J. (1997b). Aux/IAA proteins repress expression of reporter genes containing natural and highly active synthetic auxin response elements. *Plant Cell* **9**, 1963-1971.
Ulmasov, T., Hagen, G. and Guilfoyle, T. J. (1999). Dimerization and DNA binding of auxin response factors. *Plant J.* **19**, 309-319.
Wang, H., Jones, B., Li, Z., Frasse, P., Delalande, C., Regad, F., Chaabouni, S., Latche, A., Pech, J. C. and Bouzayen, M. (2005). The tomato Aux/IAA transcription factor IAA9 is involved in fruit development and leaf morphogenesis. *Plant Cell* **17**, 2676-2692.
Weijers, D., Sauer, M., Meurette, O., Friml, J., Ljung, K., Sandberg, G., Hooykaas, P. and Offringa, R. (2005). Maintenance of embryonic auxin distribution for apical-basal patterning by PIN-FORMED-dependent auxin transport in Arabidopsis. *Plant Cell* **17**, 2517-2526.
Weijers, D., Schlereth, A., Ehrismann, J. S., Schwank, G., Kientz, M. and Jurgens, G. (2006). Auxin triggers transient local signaling for cell specification in Arabidopsis embryogenesis. *Dev. Cell* **10**, 265-270.
Wenzel, C. L., Schuetz, M., Yu, Q. and Mattsson, J. (2007). Dynamics of MONOPTEROS and PIN-FORMED1 expression during leaf vein pattern formation in Arabidopsis thaliana. *Plant J.* **49**, 387-398.
Wilmoth, J. C., Wang, S., Tiwari, S. B., Joshi, A. D., Hagen, G., Guilfoyle, T. J., Alonso, J. M., Ecker, J. R. and Reed, J. W. (2005). NPH4/ARF7 and ARF19 promote leaf expansion and auxin-induced lateral root formation. *Plant J.* **43**, 118-130.
Xu, J., Hofhuis, H., Heidstra, R., Sauer, M., Friml, J. and Scheres, B. (2006). A molecular framework for plant regeneration. *Science* **311**, 385-388.
Zhang, C., Gong, F. C., Lambert, G. M. and Galbraith, D. W. (2005). Cell type-specific characterization of nuclear DNA contents within complex tissues and organs. *Plant Methods* **1**, 7.
Zhou, G. K., Kubo, M., Zhong, R., Demura, T. and Ye, Z. H. (2007). Overexpression of miR165 affects apical meristem formation, organ polarity establishment and vascular development in Arabidopsis. *Plant Cell Physiol.* **48**, 391-404.